Covariance of Meiyu Front and Tropospheric Jet Variability on Daily and Interannual time scales

Jesse A. Day,[1] Jacob Edman,[1] Inez Fung[1], and Weihan Liu[1]

Corresponding author: Jesse Day, University of California Berkeley, Department of Earth and Planetary Science, College of Letters and Science; 307 McCone Hall, Berkeley, CA 94720, USA. (jessed@berkeley.edu)

[1]Department of Earth and Planetary Science, University of California Berkeley, Berkeley, California, USA.

This abstract must be 150 words or less. The contents of the abstract count towards the total word count.

1. Introduction

China receives about 60% of its rainfall from May to August, known collectively as the East Asian summer monsoon. The period of peak rainfall within this monsoon features a northward-migrating front known as the Meiyu front (lit. "Plum rains" – capitalize front?), and lasts roughly from early June to mid-July ("Meiyu Season"). A growing volume of evidence suggests a shift in mean rainfall patterns over China beginning in the late 1970s, with increased flooding in the south and droughts in the north (the "South Flood North Drought"). A permanent change would have major humanitarian impacts on the densely-populated eastern Chinese plain, where a sizable fraction of the population depends on agriculture. The Chinese government has already embarked on a costly engineering project to reroute water from the Yangtze to the Yellow River, the South-North Water Transfer Project.

The complex atmospheric dynamics of the East Asian summer monsoon remain a source of debate [**??**]. The behavior of the Meiyu front has been discussed in the seasonal mean[**?**], and in relation to interannual rainfall variability [**?**]. However, to our knowledge, no comprehensive statistics of daily Meiyu behavior exist. We have developed an algorithm to compile a 57-year climatology (1951-2007) of frontal events in China (hereafter referred to as Meiyu events) based on the APHRODITE rain gauge product. In addition, we test the covariance of daily Meiyu behavior with that of the tropospheric jet, using an existing database from **?**. Past work has compared jet and Meiyu variability over shorter time periods or with coarse resolution**?**, but none has systematically compared the two. Finally,

given our daily Meiyu climatology, we determine whether there are apparent changes in behavior over the 57 years, and whether these also correspond to changes in jet behavior.

2. Data sets

The analysis contained in this paper relies on two data sets, APHRODITE and Schiemann et al's database of jet counts. APHRODITE (Asian Precipitation - Highly-Resolved Observational Data Integration Towards Evaluation of the Water Resources) [**?**]. The APHRO_MA_V1101 product includes 57 years (1951-2007) of daily precipitation (PRECIP product, units mm day^{-1}) and station coverage (RSTN product) on a .25° × .25° grid (roughly 25 km spacing) between 60°E-150°E and 15°S-55°N. We focus on the subregion from 100E-123E and 20N-40N as the area of occurrence of Meiyu events. Rain gauge products present an analytical challenge because the distribution of stations is uneven in space and changes with time. Station density over eastern China improves beginning in the 1970s from X to Y (INSERT ACTUAL NUMBERS). However, the spacing of stations generally does not exceed 100 km, which should be more than sufficient to resolve the macroscopic scale of a frontal event.

For tropospheric jet variability, we employ a database based on ERA-40 reanalysis data developed by **?**. Their database includes every appearance of a tropospheric jet in East Asia for 1958-2001 at 6-hourly intervals using simple criteria: Positive zonal wind and local maximum in excess of 30 m/s. We have modified Schiemann et al.'s algorithm in several respects: ...

.

3. Meiyu Climatology

3.1. Algorithm

List version

For each day from 1 January 1951 to 31 December 2007 (20,819 total), the algorithm determines whether a frontal event is present or not inside the window of 105-123E and 20-40N, and if it exists returns its properties. In addition, it is observed that some days feature two frontal events. If a primary event is detected, the algorithm therefore checks for a secondary fit as well. The algorithm follows the subsequent checklist:

1. The maximum daily rainfall for each longitude is found. If there exists a 5°continuous chain of maxima (20 points in a row) exceeding 10 mm/day, we proceed to step 2 and attempt a fit. Otherwise, the day is thrown out.

2. A weighted least-squares linear fit of the *latitudes* of the maxima is attempted, using the intensity of the maxima as weight.

3. A recursive algorithm converges on a best estimate. In each iteration, we find a new set of maxima within k degrees of the previous best fit line, and again repeat the weighted linear fit in step 2. k is progressively decreased with each iteration.

4. Using our final best estimate from step 3, we define the "quality score" Q as the fraction of total daily precipitation that falls within 5 degrees of this fit line.

5. As mentioned, we check for a secondary front. We remove all precipitation within the primary front and again apply the front criterion in step 1 to the leftover rainfall map. If passed, steps 2-4 are repeated to find a best estimate for a secondary front.

6. If a secondary front is found, two additional quality scores Q_1 and Q_2 are determined. Q_1 is defined as the fraction of rainfall contained in the primary front *after removing all rainfall associated with the secondary front.* Likewise Q_2 is the Q score of the second front after removing all rainfall from the primary front.

In some cases, a fit will be achieved, but its quality will be too poor to include in our statistics. To check for this scenario, we use the quality scores Q, Q_1 and Q_2, and the "Taiwan fraction" (TW), defined as the percentage of daily rainfall that falls on the island of Taiwan. If $TW > 20\%$, the day is thrown out. Such days are dominated by a local storm reaching Taiwan and rarely exhibit a strong front. Subsequently there are two ways a day may be included:

1. if $Q > .6$, the day is included in our statistics. If Q_2 also is greater than .6, the day will be classified as a double front day.

2. If $Q < .6$, a day can only be included if both Q_1 **and** $Q_2 > .6$. In such cases, the quality of fit is initially obscured by the presence of multiple fronts. We classify the day as a double front day.

In practice, days with secondary fronts constitute a small fraction of all days ($> 5\%$) but are more common during certain seasons.

Paragraph version

For each day from January 1 1951 to December 31 2007 (20,819 days at all) we determine whether there is a frontal event, whether there is an additional secondary front, and the characteristics of each. To detect a front, we find the maximum daily rainfall at each longitude inside the window 105-123°E and 20-40°N. If a 5°continuous chain of maxima

exceeds 10 mm/day, we seek a fit; otherwise the day is discarded. The fitting algorithm performs a linear least-squares fit of the *latitudes* of each of the maxima, weighted by the intensity of the maximum. Next, we use a recursive fit wherein we find a new set of maxima, requiring that they be within n degrees of the previous best fit line. n is progressively decreased to tighten the window and converge on an optimal fit. Given this fit, we can calculate a quality score Q, which is the percentage of total rainfall in our window that falls within 5 degrees of our best fit line. A score of $Q > .6$ constitutes a good score, as further explained below.

In addition, we determine from observation that some days feature two separate bands of strong rainfall. We would like to include such events. Therefore, after fitting a primary event, we check for a secondary event by removing the rainfall associated with the first best fit line, and then repeating all of the steps of the previous paragraph. If a secondary event is detected, we may define two extra quality scores Q_1 and Q_2, where Q_1 is the percentage of rainfall within *after removing rainfall associated with the secondary fit*, and Q_2 likewise is the Q score of the secondary fit after removing rainfall from the primary fit.

Finally, in some cases our front criterion will be satisfied, but we are not able to achieve a good fit. We use the quality scores Q, Q_1 and Q_2 to check for this case, as well as one additional metric, the "Taiwan fraction" (TW), defined as the percentage of daily rainfall that falls on Taiwan. First of all, all days where $TW > 20\%$ are thrown out. Such days are dominated by a local storm reaching Taiwan, and rarely exhibit a coherent front. Subsequently there are two ways a day may be included:

1. if $Q > .6$, the day is included in our statistics. If Q_2 also is greater than .6, the day will be classified as a double front day.

2. If $Q < .6$, a day can only be included if both Q_1 **and** $Q_2 > .6$. In such cases, the quality of fit is initially obscured by the presence of multiple fronts. We classify the day as a double front day.

In practice, days with secondary fronts constitute a small fraction of all days ($> 5\%$) but are more common during certain seasons.

3.2. Defining Meiyu season

Figure 1 shows a Hövmoller diagram of latitudes occupied by the Meiyu Front in the 57-year mean. Four local maxima of Meiyu events can be observed: 1) A "pre-Meiyu" from May 1-31 over southern China (Ding and Chan's first position); 2) Meiyu Season, in which the preferred latitude of the front shifts by almost ten degrees from June 1-July 15 (Ding and Chan stage 2); 3) A "post-Meiyu" of persistent 4) Cyclone season over Southern China. The storms during season 4 can be distinguished from earlier Meiyu events in southern China because their propagation direction is westward, opposite to eastward Meiyu storms. The combination of stages 3 and 4 corresponds to the third stage of the Meiyu in Ding and Chan, but only the core of Meiyu season (their stage 2) features significant front migration. Figure 2 shows that even in winter, rainfall events in China tend to be frontal, but their frequency increases up to almost 100% during Meiyu Season, and a surge in intensity can be seen around June 1 where mean rainfall along the front exceeds 25 mm/day. The mean tilt of the front is approximately 8 degrees.

It can be seen that mean rainfall and Meiyu occurrence are not entirely equivalent, since the Southern China peak in August does not correspond to a surge in Meiyu events.

4. Preferred jet positions

-¿ The westerly jet and rainfall are argued to covary on paleoclimate timescales [**?**][**?**].

Monthly changes in the position of the jet have previously been reported in **?**, and we do not repeat them here. It is worth noting that the pre-Meiyu in May corresponds to a time of great jet variability, whereas June features a discernible but meandering jet, and the post-Meiyu corresponds to very low variability in jet position during July and August.

Finally, we use our knowledge of daily Meiyu positions to isolate preferred configurations for different dates, as well as probability distributions of the tropospheric jet associated with each configuration. If a robust change in mean jet progression is detected, we may be able to isolate a corresponding shift in Meiyu distribution that may have previously gone unnoticed due to extreme temporal variability in the data.

We first attempt to define a transition date from spring to summer behavior in the jet database, and equivalently from Meiyu Season to post-Meiyu in our new catalog. Preliminary evidence suggests a long-term perturbation in mean jet path in East Asia from the 1960s to present with later onset of summer jet and shorter total duration of summer jet. In our Meiyu database it is more difficult to extract an exact transition date due to high-frequency variability in space and time. However, we observe an apparent shift in the timing of northward progression of the Meiyu Front between 1951-1970 and 1988-2007. If both databases demonstrate a robust decadal shift, they may provide an explanation for the anecdotal South Wet-North Dry pattern of rainfall change.

5. Covariance of jet and Meiyu anomalies

6. Dynamics

The covariance of Meiyu front positions and tropospheric jet latitudes previously demonstrated also clarifies a dynamical reason for their seasonality. As shown, Meiyu season consists of intense rainfall from June 1st to July 1st with a shift in latitude of almost 10 degrees over the course of that month. After . The lens of forced convergence by the Tibetan Plateau. In the climatological mean, **?** demonstrated that the Meiyu front exists primarily due to forced mechanical convergence by the Tibetan Plateau upstream. They showed this by using experiments in which the Tibetan Plateau's height was reduced by 95%. We argue that our results similarly show the role of the Tibetan Plateau in generating a strong Meiyu front. When the jet impinges on the Tibetan Plateau from late May to early July, the high topography induces meanders that force standing waves in jet configuration, pushing it further north from 80E to 100E and then further south into China. This in turn anchors strong rainfall along the Meiyu front in China. When the jet moves further north to its preferred summer position, which occurs just north of the Tibetan Plateau, it is no longer deflected and the front is significantly weaker, though events do still occur as seen in Figure 1. We confirm this hypothesis by showing the climatology of precipitable water vapor from SSRI from time A, time B, time C and time D (last figure). During the early and late stages of Meiyu season precipitable water content is concentrated along bands that intersect central China. However, in July and August, the latitude of the moisture vapor front has shifted much further north, over northern China, and both the Bay of Bohai and the Korean Peninsula and Japan all have much greater

precipitable water. However, the lack of mechanical forcing is shown by the weakness of rainfall in those events (<20 mm/day versus 25-30 mm/day over southern and central China during Meiyu season.

7. Conclusion

Since the behavior of the jet is coupled to global climate variability, our work holds the promise of attributing the regional rainfall trend in China to global-scale change.

-¿ Existing templates for precipitation changes under warming ([**?**][**?**][**?**]) are not easily applied to the East Asian monsoon

Acknowledgments. APHRODITE is...

References

Chen, J., and S. Bordoni (2014), Orographic Effects of the Tibetan Plateau on the East Asian Summer Monsoon: An energetic perspective, *J. Climate*, p. 140113153908002, doi:10.1175/JCLI-D-13-00479.1.

Chou, C., J. D. Neelin, C.-A. Chen, and J.-Y. Tu (2009), Evaluating the rich-get-richer mechanism in tropical precipitation change under global warming, *J. Climate*, *22*(8), 1982–2005, doi:10.1175/2008JCLI2471.1.

Ding, Y., and J. C. L. Chan (2005), The East Asian summer monsoon: an overview, *Meteorol. Atmos. Phys.*, *89*(1-4), 117–142, doi:10.1007/s00703-005-0125-z.

Held, I., and B. Soden (2006), Robust responses of the hydrological cycle to global warming, *J. Climate*, *19*(21), 5686–5699.

187 Liang, X., and W. Wang (1998), Associations between China monsoon rainfall and tro-
188 pospheric jets, *Q. J. R. Meteorol. Soc.*, *124*(May), 2597–2623.

189 Lintner, B., and J. D. Neelin (2007), A prototype for convective margin shifts, *Geophys.*
190 *Res. Lett.*, *34*(5), L05,812, doi:10.1029/2006GL027305.

191 Nagashima, K., R. Tada, A. Tani, Y. Sun, Y. Isozaki, S. Toyoda, and H. Hasegawa (2011),
192 Millennial-scale oscillations of the westerly jet path during the last glacial period, *J.*
193 *Asian Earth Sci.*, *40*(6), 1214–1220, doi:10.1016/j.jseaes.2010.08.010.

194 Nagashima, K., R. Tada, and S. Toyoda (2013), Westerly jet-East Asian summer monsoon
195 connection during the Holocene, *Geochemistry, Geophys. Geosystems*, *14*(12), 5041–
196 5053, doi:10.1002/2013GC004931.

197 Roe, G. (2009), On the interpretation of Chinese loess as a paleoclimate indicator, *Quat.*
198 *Res.*, *71*(2), 150–161, doi:10.1016/j.yqres.2008.09.004.

199 Sampe, T., and S.-P. Xie (2010), Large-Scale Dynamics of the Meiyu-Baiu Rain-
200 band: Environmental Forcing by the Westerly Jet, *J. Climate*, *23*(1), 113–134, doi:
201 10.1175/2009JCLI3128.1.

202 Schiemann, R., D. Lüthi, and C. Schär (2009), Seasonality and Interannual Variability
203 of the Westerly Jet in the Tibetan Plateau Region, *J. Climate*, *22*(11), 2940–2957,
204 doi:10.1175/2008JCLI2625.1.

205 Yatagai, A., K. Kamiguchi, O. Arakawa, A. Hamada, N. Yasutomi, and A. Kitoh (2012),
206 APHRODITE: Constructing a Long-Term Daily Gridded Precipitation Dataset for Asia
207 Based on a Dense Network of Rain Gauges, *Bull. Am. Meteorol. Soc.*, *93*(9), 1401–1415,
208 doi:10.1175/BAMS-D-11-00122.1.

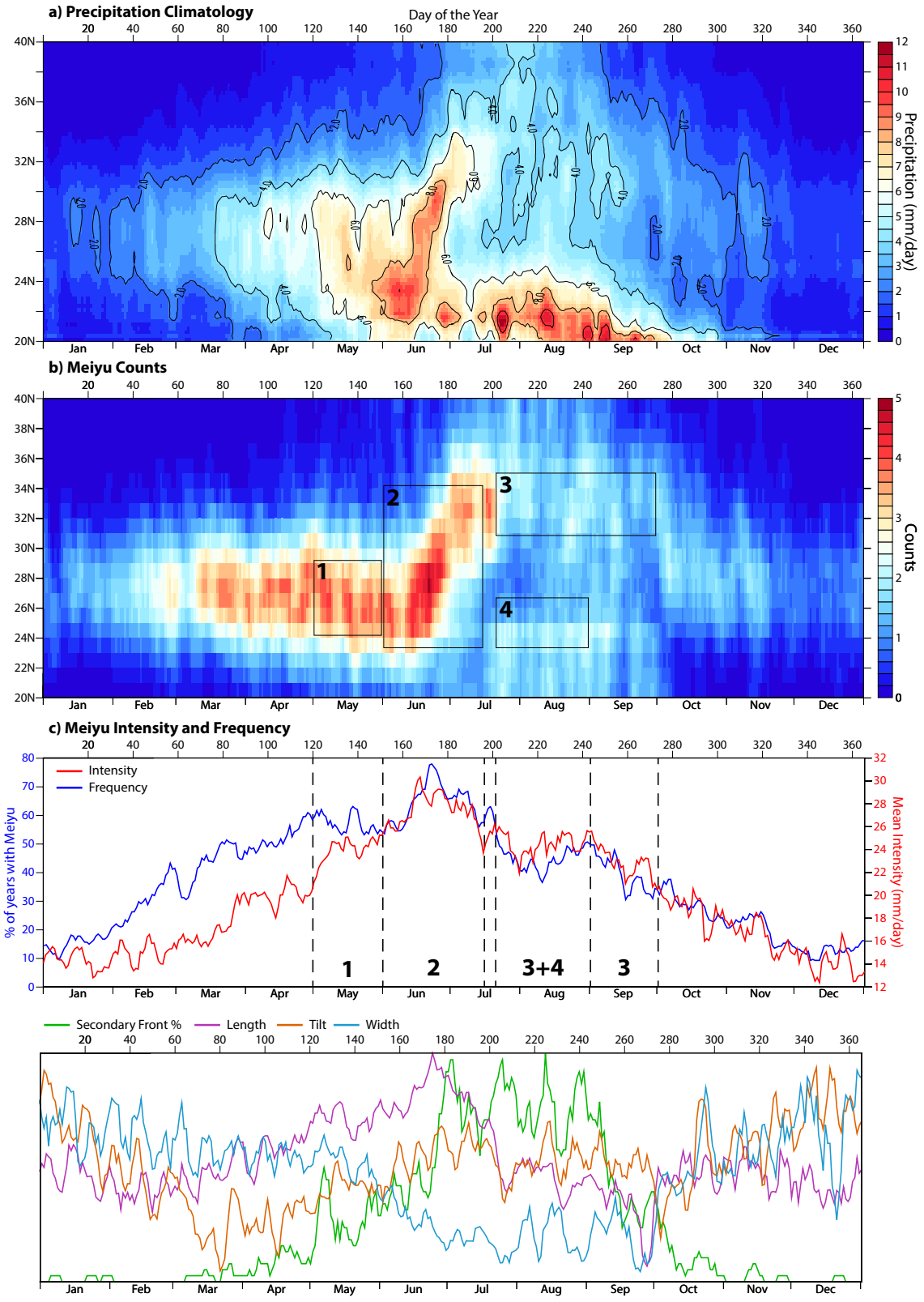

Figure 1. Climatology of the Meiyu Front, 1951-2007. 1) Pre-Meiyu 2) Meiyu 3) Cyclone season in Southern China 4) Storms advected by summer jet